10-2011

Quantified H i morphology – IV. The merger fraction and rate in WHISP.

Benne W. Holwerda
University of Louisville

N. Pirzkal
Space Telescope Science Institute

W. J. G. de Blok
University of Cape Town

A. Bouchard
McGill University

S. -L. Blyth
University of Cape Town

See next page for additional authors

Original Publication Information

Authors

Benne W. Holwerda, N. Pirzkal, W. J. G. de Blok, A. Bouchard, S. -L. Blyth, and K. J. van der Heyden

Quantified H I morphology – IV. The merger fraction and rate in WHISP

B. W. Holwerda,[1,2]★ N. Pirzkal,[3] W. J. G. de Blok,[2] A. Bouchard,[4] S.-L. Blyth[2] and K. J. van der Heyden[2]

[1]*European Space Agency, ESTEC, Keplerlaan 1, 2200 AG, Noordwijk, the Netherlands*
[2]*Astrophysics, Cosmology and Gravity Centre (ACGC), Astronomy Department, University of Cape Town, Private Bag X3, 7700 Rondebosch, Republic of South Africa*
[3]*Space Telescope Science Institute, 3700 San Martin Drive, Baltimore, MD 21218, USA*
[4]*Department of Physics, Rutherford Physics Building, McGill University, 3600 University Street, Montreal, Quebec, H3A 2T8, Canada*

ABSTRACT

The morphology of the atomic hydrogen (H I) disc of a spiral galaxy is the first component to be disturbed by a gravitational interaction such as a merger between two galaxies. We use a simple parametrization of the morphology of H I column density maps of the Westerbork observations of neutral Hydrogen in Irregular and SPiral galaxies (WHISP) project to select those galaxies that are likely undergoing a significant interaction. Merging galaxies occupy a particular part of parameter space defined by Asymmetry (A), the relative contribution of the 20 per cent brightest pixels to the second-order moment of the column density map (M_{20}) and the distribution of the second-order moment over all the pixels (G_M).

Based on their H I morphology, we find that 13 per cent of the WHISP galaxies are in an interaction (Concentration–M_{20}) and only 7 per cent are based on close companions in the data cube. This apparent discrepancy can be attributed to the difference in visibility time-scales: mergers are identifiable as close pairs for 0.5 Gyr but are identifiable for ∼1 Gyr by their disturbed H I morphology. Expressed as volume merger rates, the two estimates agree very well: 7 and 6.8×10^{-3} mergers Gyr^{-1} Mpc^{-3} for paired and morphologically disturbed H I discs, respectively.

The consistency of our merger fractions with those published for bigger surveys such as the Sloan Digital Sky Survey shows that H I morphology can be a very viable way to identify mergers in large H I surveys. The relatively high value for the volume merger rate may be a bias in the selection or WHISP volume. The expected abundance in high-resolution H I data by the planned South African Karoo Array Telescope (MeerKAT), Australian SKA Pathfinder (ASKAP) and Westerbork Synthesis Radio Telescope/APERture Tile In Focus instrument (WSRT/APERTIF) radio observatories will reveal the importance of mergers in the local Universe and, with the advent of the Square Kilometer Array (SKA), over cosmic times.

Key words: galaxies: fundamental parameters – galaxies: interactions – galaxies: kinematics and dynamics – galaxies: spiral – galaxies: structure.

1 INTRODUCTION

Merger of galaxies is a driving factor in galaxy evolution over cosmic times. Several schemes to identify merging galaxy pairs have been developed in the past decade, many based on the number of physically close pairs (in both sky coordinates and redshift) or on the characterization of the disturbed appearance of galaxies due to gravitational interaction (often through visual inspection, e.g. Arp 1973; Vorontsov-Velyaminov, Noskova & Arkhipova 2001; Darg et al. 2010). Both these techniques have been used to determine

the interaction fraction in the local Universe as well as out to high redshift in *Hubble* images. Using *N*-body simulations, one can determine for how long a merger will be identified by either technique: i.e. for how long the galaxy pair will be close enough, or for how long the galaxies look sufficiently disturbed.

Because the volume probed increases with redshift, there were until recently – paradoxically – better measures of the interaction fraction for higher redshift than for the local Universe. The Sloan Digital Sky Survey (SDSS) search for close (and disturbed looking) pairs of galaxies (Darg et al. 2010) added the valuable local Universe interaction fraction, improving on the estimate by Patton et al. (1997) from close pairs in the Uppsala General Catalogue

★ E-mail: benne.holwerda@esa.int
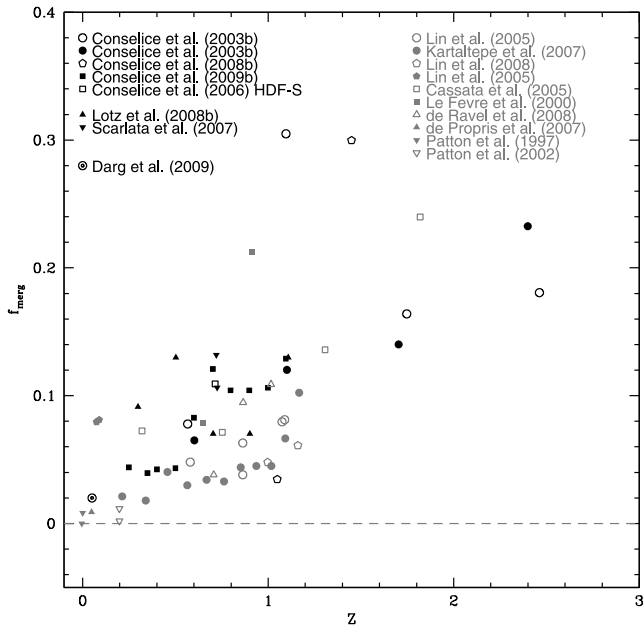
Figure 1. The merger fraction (f_{merg}) as a function of redshift (z). The black points are based on quantified morphology estimates, and the grey points are based on galaxy pair counts. The Conselice et al. papers are based purely on the CAS classification system; Lotz et al. (2008) use the Gini/M_{20} classification and Scarlata et al. (2007) use both the CAS and the Gini and M_{20} parameters. The results by De Propris et al. (2007a) and Darg et al. (2010) are hybrid approaches: De Propris et al. (2007a) look at not only pair statistics but also galaxy asymmetry, and Darg et al. (2010) used the visual identification of a merging pair in the Galaxy Zoo project (Lintott et al. 2008). See Table 1 for the data sets used and the references.

(Nilson 1973). A compilation of merger fractions determined as a function of redshift is shown in Fig. 1 and Table 1. The scatter in the merger fractions, even for those determined over the same data, is striking and it is tied to the definition of what constitutes a pair or disturbed morphology (see e.g. the discussion in Genel et al. 2009). The definition of morphologically disturbed became quantified in several schemes of morphological parametrization (e.g. Conselice

Table 1. The references, data sets and methods for merger fractions in the local and distant Universe.

Reference	Data set	Criteria
Morphology		
Conselice et al. (2003)	HDF-N	CAS
Conselice et al. (2008)	HUDF	CAS
Conselice, Yang & Bluck (2009)	EGS, COSMOS	CAS
Conselice, Blackburne & Papovich (2005)	HDF-S	CAS
Lotz et al. (2008)	EGS	G/M_{20}
Scarlata et al. (2007)	COSMOS	CAS + G/M_{20}
Pair statistics:		
Lin et al. (2004)	DEEP2	
Lin et al. (2008)	DEEP2	
Kartaltepe et al. (2007)	COSMOS	
de Ravel et al. (2009)	VLT/DEEP	
Cassata et al. (2005)	GOODS	
Le Fèvre et al. (2000)	CFRS, *HST*	
Patton et al. (1997)	CNOC1	
Patton et al. (2002)	CNOC2	
De Propris et al. (2007a)	MGC	

2003; Lotz, Primack & Madau 2004). Observational uncertainties are the time-scale over which a merger is identifiable as such, the completeness of the various samples for each technique and the volumes considered. Similarly, a current substantial theoretical effort is to map the dark matter halo merger rates on to actual observable galaxy mergers (Hopkins et al. 2010, and reference therein).

The morphological studies are largely based on optical, mostly *B*-band and rest-frame ultraviolet (UV) data. The reasoning goes that mergers trigger star formation and the resulting increased surface brightness makes the disturbed morphology of the galaxy easier to identify (although the increase in star formation is not a certainty; see Robaina et al. 2009). However, with the emergence of new and refurbished radio observatories in preparation for the future Square Kilometer Array (SKA; Carilli & Rawlings 2004), a new window on merger rates over cosmic times will be opening up: the 21 cm emission line of atomic hydrogen gas (H I). The two SKA precursors, the South African Karoo Array Telescope (MeerKAT; Jonas 2007; Booth et al. 2009; de Blok et al. 2009), and the Australian SKA Pathfinder (ASKAP; Johnston 2007; Johnston et al. 2007, 2008; Johnston, Feain & Gupta 2009) stand poised to observe a large number of Southern Hemisphere galaxies in H I in the nearby Universe ($z < 0.2$). In addition, the Extended Very Large Array (EVLA; Napier 2006) and the APERture Tile In Focus instrument (APERTIF; Verheijen et al. 2008; Oosterloo et al. 2009) on the Westerbork Synthesis Radio Telescope (WSRT) will do the same for the Northern Hemisphere. The advantage of H I observation is that it contains both morphological and kinematic information on spiral discs. There is ample anecdotal evidence of disturbed H I morphology during a merger (see the compilation in Hibbard et al. 2001).[1] In this series of papers, we primarily explore the signature of gravitational interaction on the morphology of the (face-on) H I disc. This is a suitable complement to any kinematic signature, which will be most clear in edge-on discs. Our motivation to move to the H I perspective is that (a) the gas will be disturbed before the stellar disc, (b) the H I morphology will be more sensitive to minor interactions, which may dominate the number of interactions, and (c) the H I morphology will be intrinsically sensitive to gas-rich interactions. Minor and gas-rich interactions are expected to dominate at higher redshift, which makes an H I perspective at low redshift a good local comparison.

In the previous papers in this series, we compared the H I morphology to that at other wavelengths (Holwerda et al. 2009, 2011b) and found it to be at least as good a tracer of mergers as any other wavelength. We defined an H I parameter space to identify interacting galaxies (Holwerda et al. 2011c) and derived a time-scale for interactions to reside in this parameter space (this paper's companion; Holwerda et al. 2011d). In this paper, the aim is to combine the morphological identification of mergers with the time-scales into a merger fraction and rate for the Westerbork observations of neutral Hydrogen in Irregular and SPiral galaxies (WHISP) sample. This paper is organized as follows. In Section 2 we briefly describe the morphological parameters and selection criteria; in Section 3 we discuss the limitations and applicability of these in the context of H I data. In Section 4, Sections 4.1 and 4.2 describe the WHISP basic data and H I column density maps. In Section 4.3 we derive the volume representative for the WHISP survey. In Section 5, we derive the merger fraction based on the number of pairs as well as the morphology and convert these into merger rates in Section 6. Sections 7 and 8 are our discussion and conclusions.

---

[1] The H I Rogues Gallery: http://www.nrao.edu/astrores/HIrogues/

2 MORPHOLOGICAL PARAMETERS AND MERGER CRITERIA

In this series we use the Concentration–Asymmetry–Smoothness (CAS) parameters (Conselice 2003), combined with the Gini–M_{20} parameters from Lotz et al. (2004) and one addition of our own, G_M. We discussed the definitions of these parameters in the previous papers, as well as how we estimate uncertainties for each. Briefly, given a set of n pixels in each object, iterating over pixel i with value I_i, position x_i, y_i with the centre of the object at x_c, y_c, these parameters are defined as

$$C = 5 \log(r_{80}/r_{20}), \tag{1}$$

with r_f as the radial aperture, centred on x_c, y_c containing percentage f of the light of the galaxy (see definitions of r_f in Bertin & Arnouts 1996; Holwerda 2005).

$$A = \frac{\Sigma_i |I_i - I_{180}|}{\Sigma_i |I(i)|}, \tag{2}$$

where I_{180} is the pixel at position i in the galaxy's image, after it was rotated 180° around the centre of the galaxy.

$$S = \frac{\Sigma_{i,j} |I(i,j) - I_S(i,j)|}{\Sigma_{i,j} |I(i,j)|}, \tag{3}$$

where I_S is pixel i in a smoothed image. The type of smoothing has changed over the years. We chose a fixed 5 arcsec Gaussian smoothing kernel for simplicity.

The Gini coefficient is defined as

$$G = \frac{1}{\bar{I} n(n-1)} \Sigma_i (2i - n - 1) I_i, \tag{4}$$

where the list of n pixels was first ordered according to value and $\bar{I}$ is the mean pixel value in the image.

$$M_{20} = \log \left(\frac{\Sigma_i M_i}{M_{tot}} \right), \quad \text{for } \Sigma_i I_i < 0.2 I_{tot}, \tag{5}$$

where M_i is the second-order moment of pixel i; $M_i = I_i \times [(x - x_c)^2 + (y - y_c)^2]$. M_{tot} is the second-order moment summed over all pixels in the object and M_{20} is the relative contribution of the brightest 20 per cent of the pixels in the object. Instead of using the intensity of pixel i, the Gini parameter can be defined using the second-order moment:

$$G_M = \frac{1}{\bar{M} n(n-1)} \Sigma_i (2i - n - 1) M_i. \tag{6}$$

These parameters trace different structural characteristics of a galaxy's image but these do not span an orthogonal parameter space (see the discussion in Scarlata et al. 2007). Originally, the above parameters were envisaged to classify the morphologies of galaxies but it was soon realized that a subspace of the parameters is occupied by gravitationally interacting late-types. Conselice (2003) and Lotz et al. (2004) introduced several different criteria for the selection of merging systems in terms of the CAS and Gini–M_{20} parameters. For optical data, Conselice (2003) define the following criterion:

$$A > 0.38, \tag{7}$$

with some authors requiring $A > S$ as well.

Lotz et al. (2004) added two different criteria using Gini and M_{20}:

$$G > -0.115 \times M_{20} + 0.384 \tag{8}$$

and

$$G > -0.4 \times A + 0.66 \quad \text{or} \quad A > 0.4, \tag{9}$$

the latter being a refinement of the Conselice et al. criterion in equation (7).

These criteria were developed for optical morphologies, typically observed in rest-frame Johnson-*B* or SDSS-*g* optical filters. Therefore, in the second paper in this series (Holwerda et al. 2011c), we defined several possible criteria specifically for the H I perspective using the CAS–G/M_{20}–G_M space of the WHISP survey H I map sample. We defined the Gini parameter of the second-order moment, G_M, and a criterion for this parameter that selected most interacting galaxies:

$$G_M > 0.6. \tag{10}$$

Earlier in this series, we speculated that a combination of Asymmetry and M_{20} could well be used to select interaction in H I morphology in Holwerda et al. (2011b). In Holwerda et al. (2011c), we defined such a criterion as

$$A > -0.2 \times M_{20} + 0.25. \tag{11}$$

Finally, we also defined one based on Concentration and M_{20}, following the example of the Lotz et al. (2004) criteria (equations 8 and 9):

$$C > -5 \times M_{20} + 3. \tag{12}$$

In Holwerda et al. (2011b), we found that this last criterion both selected the correct fraction of interacting galaxies, and agreed most often with the previous visual identifications in the case of individual WHISP galaxies. We will now explore merger rates based on the above criteria for H I morphology.

3 LIMITATIONS

Similarly to other morphological selection schemes, we note that our approach is most sensitive to mergers involving at least one gas-rich late-type galaxy for the morphological selection and two in the case of pair selection of mergers. H I observations pre-select against early-types (see Fig. 2 and Section 4.1) and the morphological disturbance is sensitive to unequal-mass mergers (cf. Lotz et al. 2010b). Therefore, this approach is complementary to existing morphological identification of mergers but dissimilar enough to warrant a separate estimate of time-scales.

In Holwerda et al. (2011d), we compared the visibility time-scales for the above criteria in the case of mergers of two equal-mass spirals to those of a secularly evolving spiral. We find that the spiral–spiral merger is visible in morphological criteria during two stages before the final coalescence into the merger remnant: once during the initial approach (before the stellar disc is disturbed) and during the second pass, before coalescence. The total visibility time is approximately a gigayear with some variance due to observation angle, different treatment of feedback from star formation on the interstellar medium (ISM) in the simulation and the relative gas fraction of the spiral disc. We note that the time-scales for selection for merging and isolated (passively evolving) H I discs become the same for resolutions coarser than the WHISP observations used here, e.g. the VLA Imaging of Virgo spirals in Atomic gas survey (VIVA; Chung et al. 2009). A limitation of the simulations used (originally from Cox et al. 2006a,b) is that they are for Milky Way sized spiral galaxies only and do not consider minor mergers. Thus, since our approach may be sensitive to some minor merger scenarios, which possibly have much shorter visibility time-scales, the inferred visibility time from Holwerda et al. (2011d) should
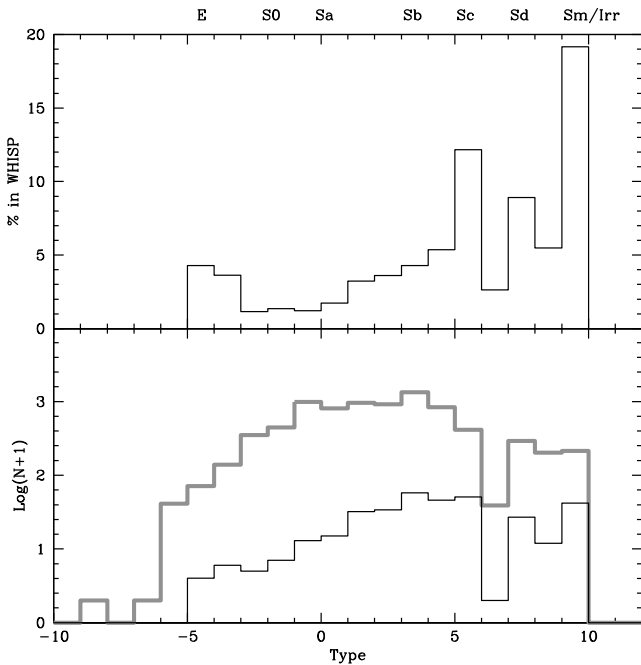
Figure 2. Bottom panel: the distribution of Hubble types in WHISP (black line) and the part of the UGC that conforms to the selection criteria for WHISP (thick grey line). Top panel: percentage of the UGC catalogue observed in WHISP as a function of type. There is a clear preference in the WHISP selection for later-type galaxies, but ellipticals are not specifically excluded and large early-types would make the H I flux cut. Hubble type determinations are from the 2MASS survey (Kleinmann et al. 1994), not the UGC.

be considered the upper limit for H I morphological selection of mergers.

In a subsequent paper (Holwerda et al. 2011e), we show that the H I morphology is also sensitive to ram pressure by a dense intergalactic medium but that one can select against this ongoing or recent stripping with the Concentration index. For the WHISP survey we find in Holwerda et al. (2011c) from a WHISP subsample and in Holwerda et al. (2011d) from simulated H I maps that the level of contamination for the above parameters varies but is acceptable for large volume studies. For example, these still are noisy H I maps in our morphological selection (see Fig. 6 and Appendix A in the electronic version of the article – see Supporting Information).

4 WHISP

The data set here comprises the observations done as part of the Westerbork WHISP project (van der Hulst, van Albada & Sancisi 2001; van der Hulst 2002). WHISP is a survey of the neutral hydrogen component in spiral and irregular galaxies with the WSRT. It has mapped the distribution and velocity structure of H I in several hundreds of nearby galaxies, increasing the number of H I observations of galaxies by an order of magnitude. The WHISP project provides a uniform data base of data cubes, zeroth-order and velocity maps. Its focus has been on the structure of the dark matter halo as a function of the Hubble type, the Tully–Fisher relation and the dark matter content of dwarf galaxies (Swaters et al. 2002a; Swaters & Balcells 2002; Noordermeer et al. 2005a). Until the large all-sky surveys with new instruments are completed, WHISP is the largest, publicly available data set of resolved H I observations. We compiled a catalogue of
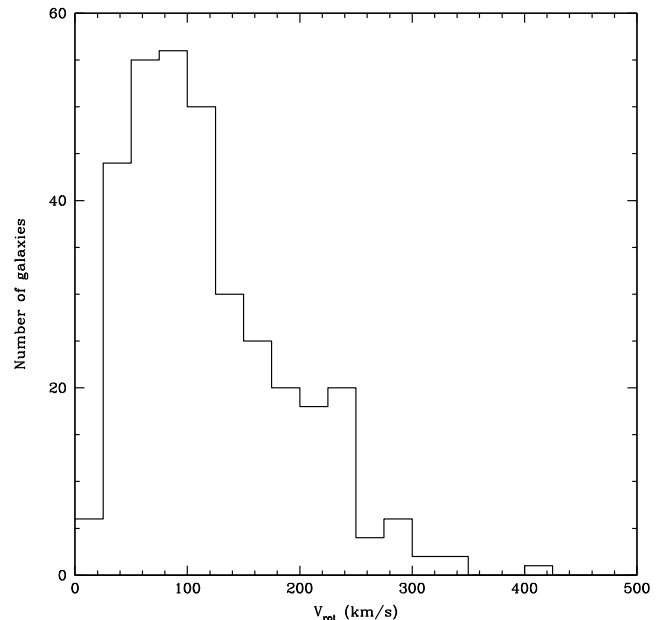
Figure 3. The distribution of rotation velocity (v_{rot}) over the complete WHISP sample.

basic data, obtained the highest available H I column density maps and estimated the representative volume of WHISP.

4.1 WHISP basic data

Basic data for the WHISP sample came from the UGC catalogue, updated from HyperLEDA (Paturel et al. 2003a). We used updated positional data, preferring, in order, the Two-Micron All-Sky Survey (2MASS) (Kleinmann et al. 1994), the updated Uppsala Galaxy Catalogue positional data (Cotton, Condon & Arbizzani 1999), the Principal Galaxy Catalogue (Paturel et al. 2003b), the original Uppsala Galaxy Catalogue positions (Nilson 1973) and finally the compilation of coordinates internal to HyperLEDA. The major and minor axes came from the same catalogues in the same order. To define a sufficient sized area around the H I disc, we multiplied the major axis with a factor of 7. This is to speed up computation and leave out a galaxy's companions in the column density maps.

For the morphological information we again relied first on the 2MASS catalogue and secondly on the Uppsala Galaxy Catalogue, and finally on any information in HyperLEDA. The redshift information is primarily from Springob et al. (2005) for many galaxies with the remaining ones filled in from a myriad of sources in HyperLEDA. Fig. 2 shows the distribution of Hubble types in the UGC and WHISP catalogues: there is a clear preference for late-types in WHISP.

We also obtained HyperLEDA values for the rotational velocity (v_{rot}). Fig. 3 shows the distribution of v_{rot} over the WHISP sample: WHISP selection prefers smaller ($v_{rot} < 120$ km s^{-1}) and more nearby systems (Fig. 4).

4.2 WHISP column density maps

The WHISP observation targets were selected from the Uppsala General Catalogue of Galaxies (Nilson 1973), with blue major axis diameters >2.0 arcmin, declination (B1950) >20° and flux densities at 21 cm larger than 100 mJy, later lowered to 20 mJy. Observation times were typically 12 h of integration. The galaxies
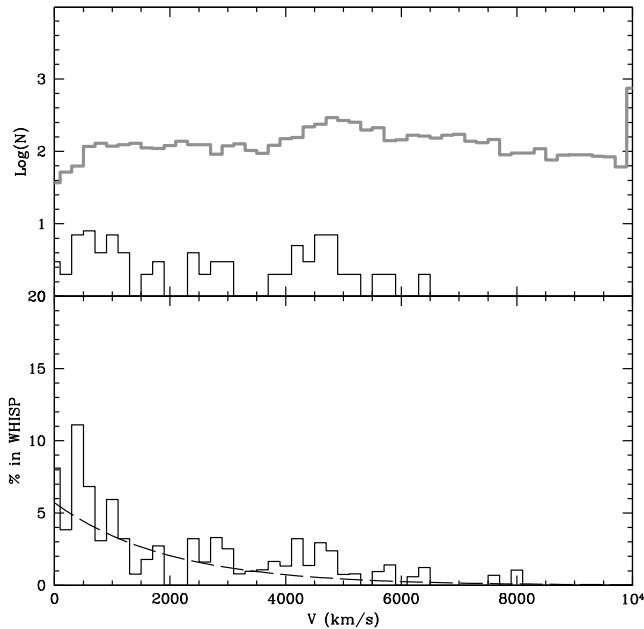
Figure 4. Top panel: the distribution of recessional velocities of the WHISP galaxies and those in the part of the UGC that conform to the selection criteria for WHISP. Bottom panel: percentage of the UGC catalogue observed in WHISP as a function of redshift. The fraction of WHISP galaxies drops off with redshift. The exponential fit to this drop-off is the dashed line, used to estimate the representative volume of the WHISP survey.

satisfying these selection criteria generally have redshifts less than $20\,000$ km s^{-1} ($z < 0.07$).

The observational criteria (see above) are in effect a selection against early-type galaxies (preferring spirals and irregulars; Fig. 2), and a preference for galaxies below $cz = 5000$ km s^{-1} (Noordermeer 2006, chapter 2). Fig. 2 shows a histogram of the Hubble types in WHISP and the same volume in the UGC. There is a preference for later-type galaxies but no exclusive selection; only a few per cent of the early types are selected and $\sim$10 per cent of the later types.

The WHISP data were retrieved from the 'Westerbork on the Web' (WOW) project at ASTRON (http://www.astron.nl/wow/). We use the column density maps with the highest resolution available [$\sim$12 × 12 arcsec^2/ sin(δ)].

4.3 The WHISP volume

A definition of the WHISP volume is not straightforward as WHISP was not meant as a complete volume-limited sample of galaxies. In the case of a *blind* H I survey, the estimate of the volume sampled is complicated by the detection function of galaxies in the observations which depends on the bandwidth, frequency resolution and threshold used in the survey (see Zwaan et al. 1997; Zwaan 2000, chapter 3). However, since WHISP is a *targeted* survey from an existing optical catalogue, we can compute the volume represented by the optical catalogue (UGC), estimate what fraction of the UGC the WHISP catalogue represents and thus what fraction of the UGC volume is representative of the WHISP survey.

Naively, the volume covered by the UGC with a declination over $20°$ and $cz < 5000$ km s^{-1} ($r = 68.5$ Mpc) is: $V_{UGC}(\delta > 20°) = (2\pi/3)\,r^2\,h = (2\pi/3)\,r^3 \times 1 - \sin(\delta) = 4.43 \times 10^5$ Mpc^3. Of the 8147 galaxies in the UGC, 339 galaxies are in WHISP; 4.17 per cent of those in the volume. However, to equate the WHISP volume to 4.17 per cent of the UGC volume (18473 Mpc^3) would be simplistic

as there is a bias towards nearby galaxies in the WHISP selection (see Fig. 4).

Fig. 4 shows the distribution in redshift of the WHISP sample and the total UGC sample ($\delta > 20°$), as well as the percentage of the UGC galaxies in WHISP. We fit an exponential distribution to the fraction and obtain the radial weighting function for the volume of the UGC corresponding to the WHISP sample: $w(r) = f_0 e^{-r/h}$ with $f_0 = 5.7$ per cent and $h = 1947$ km s$^{-1} = 27$ Mpc. To compute the WHISP volume we integrate over radius, weighting the radius with the above function: $V = \int 2\pi r h w(r)\,\mathrm{d}r = 6835$ Mpc^3, 1.5 per cent of the UGC volume. We will use this volume for our computation of volume merger rates further in this paper. Because the WHISP survey was never meant to be a volume-limited estimate, this estimate of the representative volume should be treated with caution. Fortunately, the future planned H I surveys with ASKAP and APERTIF are set to be volume-limited.

5 MERGER FRACTION

There are two ways for us to estimate the merger fraction of the WHISP sample: by counting either the number of close pairs or the number of galaxies that look disturbed.

We should note that in the lowest mass range ($M < 10^{10}$ M$_\odot$), the observed merger fractions are very high for redshift range $z = 0.2$–1.2 ($\sim$10 per cent; Bridge et al. 2007; Kartaltepe et al. 2007; Lotz et al. 2008; Lin et al. 2008; Conselice, Yang & Bluck 2009; Jogee et al. 2009; Bridge, Carlberg & Sullivan 2010). Because the WHISP selection prefers nearby, irregular and smaller systems (Figs 2, 3 and 4), one can expect a high fraction of them to be merging.

5.1 Galaxy pairs in WHISP

There are several galaxies that have a close companion in the H I data cube. Each data cube is a single WRST pointing (10 × 10 arcmin^2) with a bandwidth of 320, 680, 1280 or 2560 km s^{-1}, depending on the velocity resolution used. While this is not the typical selection criterion for pair selection (see Patton et al. 2000), we could use it as such since pairs are selected for proximity on the sky and in redshift. In the full WHISP catalogue, there are 35 galaxies with one or more companions in the WHISP cube. Naively, this translates to a close companion and hence merger fraction (f_{mgr}) of $\sim$10 per cent of the WHISP sample. The merger fraction based on the close pairs depends on how many of those galaxies with companions one would consider to be merging. Typically, the velocity difference is taken to be less than 500 km s^{-1} to constitute a merging pair, so the data cube criteria are not stringent enough. If we go by the merger qualifiers from Swaters et al. (2002b) and Noordermeer et al. (2005b), 10 of the 24 galaxies they classify and which have companions are not merging (68 per cent success rate; see Table 2). So the real merger fraction of the WHISP catalogue is closer to $\sim$7 per cent, which puts it close to the local values from Patton et al. (1997), De Propris et al. (2007a) and Darg et al. (2010) (see Fig. 1) for the local volume.

5.2 WHISP merger fraction from H I morphology

In Holwerda et al. (2011c), we identified the part of morphology parameter space that contains a representative number of the merging galaxies in a subsample of the WHISP data base for which we had visual classifications of interaction using the H I maps from either Swaters et al. (2002b) or Noordermeer et al. (2005b). Based on a plot similar to that of Fig. 5, we concluded that criteria based on Asymmetry, M_{20}, Concentration and G_M selected the correct

Galaxy	Companions	Int?	Ref
UGC 624	2	Y	NM05
UGC 1437	1	–	–
UGC 2141	1	N	NM05
UGC 2154	Multiple	y	NM05
UGC 2459	1	–	–
UGC 2487	2	N	NM05
UGC 2916	2	Y	NM05
UGC 2941	1	Y	NM05
UGC 2942	1 (UGC 2943)	–	–
UGC 3205	3	N	NM05
UGC 3382	1	N	NM05
UGC 3384	1	–	–
UGC 3407	3	Y	NM05
UGC 3426	1	Y	NM05
UGC 3546	1	N	NM05
UGC 3642	1	Y	NM05
UGC 3698	1	N	SW02
UGC 4458	1	Y	NM05
UGC 4666	1	N	NM05
UGC 4806	Multiple	–	–
UGC 5060	1	N	NM05
UGC 5935	Multiple	y	SW02
UGC 6001	1	N	NM05
UGC 6787	1	Y	NM05
UGC 7183	1	–	–
UGC 7353	1	–	–
UGC 7506	1	N	NM05
UGC 7989	1	Y	NM05
UGC 8271	3	Y	NM05
UGC 9642	1	–	–
UGC 9858	1	–	–
UGC 10791	2	–	–
UGC 11283	1	–	–
UGC 11951	1	Y	NM05
UGC 12815	Multiple	Y	NM05

fraction of interacting galaxies in a given sample (equations 10–12). Especially in the case of the Concentration–M_{20} selection, not only did we obtain the same fraction of interaction, but this criterion agreed with the majority of the visual classification of the H I map in individual cases. In a companion paper in this series (Holwerda et al. 2011d), we explored how long both these criteria and those from the literature (equations 7–9) select mergers by their H I morphology.

We can now apply these selection criteria to the full WHISP sample. The values for the morphological parameters of the full WHISP sample are listed in Table A1 in the Appendix (see Supporting Information). Table 3 summarized our results for morphological selection for each of the six criteria: the fraction of the total WHISP sample selected, the resulting volume density, the visibility time-scale from Holwerda et al. (2011d) and the computed volume merger rates. For comparison, it also shows the values for the merger selection based on close pairs computed above. Fig. 5 shows the parameter space highlighting those selected by the Concentration–M_{20} criterion. We excluded those galaxies with $A = 1$, as this extreme value is indicative of an incorrect central position (x_c, y_c) of the WHISP galaxy

from HyperLEDA. Starting with the best performing selection criterion (equation 12), we find that 45 galaxies out of the 339 in the WHISP catalogue are interacting, or 13 per cent. The other selection criteria select much higher fractions. The next best performing criterion (G_M) selected mergers very cleanly in the *N*-body simulations but its time-scale appears to be very resolution sensitive. The Concentration–M_{20} criterion selected these 45 galaxies based on their H I morphology but we do not expect each to be a merger individually (see Fig. 6 for some examples from the selection. All the H I contour maps are shown in Fig. A1 overplotted on the 2MASS-*K* images). Close to the selection criterion (dotted line in Fig. 5, panel IX), individual measures may scatter in and out of the selection. However, based on our experience in Holwerda et al. (2011c), the fraction of mergers in WHISP is correct and individual galaxies are likely to be interacting viewed in the H I perspective. Often their optical appearance may be still undisturbed as these are in the earliest stages of the merger.[2] From the morphologies of the selected galaxies (see Fig. 6 and the Appendix in the electronic version of the article), one can see that some noisy maps are still selected as well. A more uniform (pipeline-reduced) survey will suffer less from these spurious selections.

The merger fraction we find from H I morphology selection is higher than those that other authors find for the local Universe; for example, Darg et al. (2010) find 1–3 per cent of all galaxies in SDSS to be merging and Patton et al. (2002) similarly find only a few per cent from galaxy pairs. However, our fraction is similar to those found at slightly higher redshifts ($z \sim 0.1$; see Fig. 1). As pointed out in Section 4, the H I morphology selection is likely sensitive to some minor merger scenarios as well. Minor mergers are expected to dominate the number of ongoing mergers and could in part explain our higher fraction.

6 WHISP VOLUME MERGER RATE

From the number of galaxies with a companion or the number of disturbed looking galaxies in a given volume (n_c and n_{dist}, respectively), one can calculate the volume merger rate (R_{mgr}), provided one has an estimate of the merger time-scale (T_{mgr}), the merger rate from pairs, $R_{mgr}(\text{pairs}) = n_c/T_{mgr}(\text{pairs})$ or the merger rate from morphology $R_{mgr}(\text{morph}) = n_{dist}/T_{mgr}(\text{morph})$. From Holwerda et al. (2011d), we have an estimate of the *mean* merger time-scale with some variance due to differences in merger conditions (type of feedback physics in interstellar matter, type of encounter and gas masses of the discs) and perspective (face-on versus edge-on). Lotz et al. (2010a,b) similarly note that time-scales depend on mass ratio and gas fraction for optical morphological selection.

Mergers were on average visible for 40 per cent of the 2.5 Gyr of the merger simulation, making our typical time-scale $T_{mgr}(\text{morph})$ $\sim$ 1 Gyr (see Holwerda et al. 2011d), very similar to those used in the literature for morphological selection. Patton et al. (2000) and Patton & Atfield (2008) use a merger time-scale for pairs of $T_{mgr}(\text{pairs}) = 0.5$ Gyr. The volume represented by the WHISP sample was computed above (Section 4.3) as 6835 Mpc^3.

Following our simple merger fraction of 7 per cent from the number of WHISP galaxies with companions in the data cube, we obtain a volume merger rate of $R_{mgr}(\text{pairs}) = 0.7 \times 10^{-2}$ mergers Mpc^{-3} Gyr^{-1}. Merger rates based on H I morphology can use a

---

[2] See also the H I Rogues Gallery for many examples of disturbed H I morphology in normal appearing spirals: http://www.nrao.edu/astrores/HIrogues/RoguesLiving.shtml (Hibbard et al. 2001).

Morphology Parameterspace
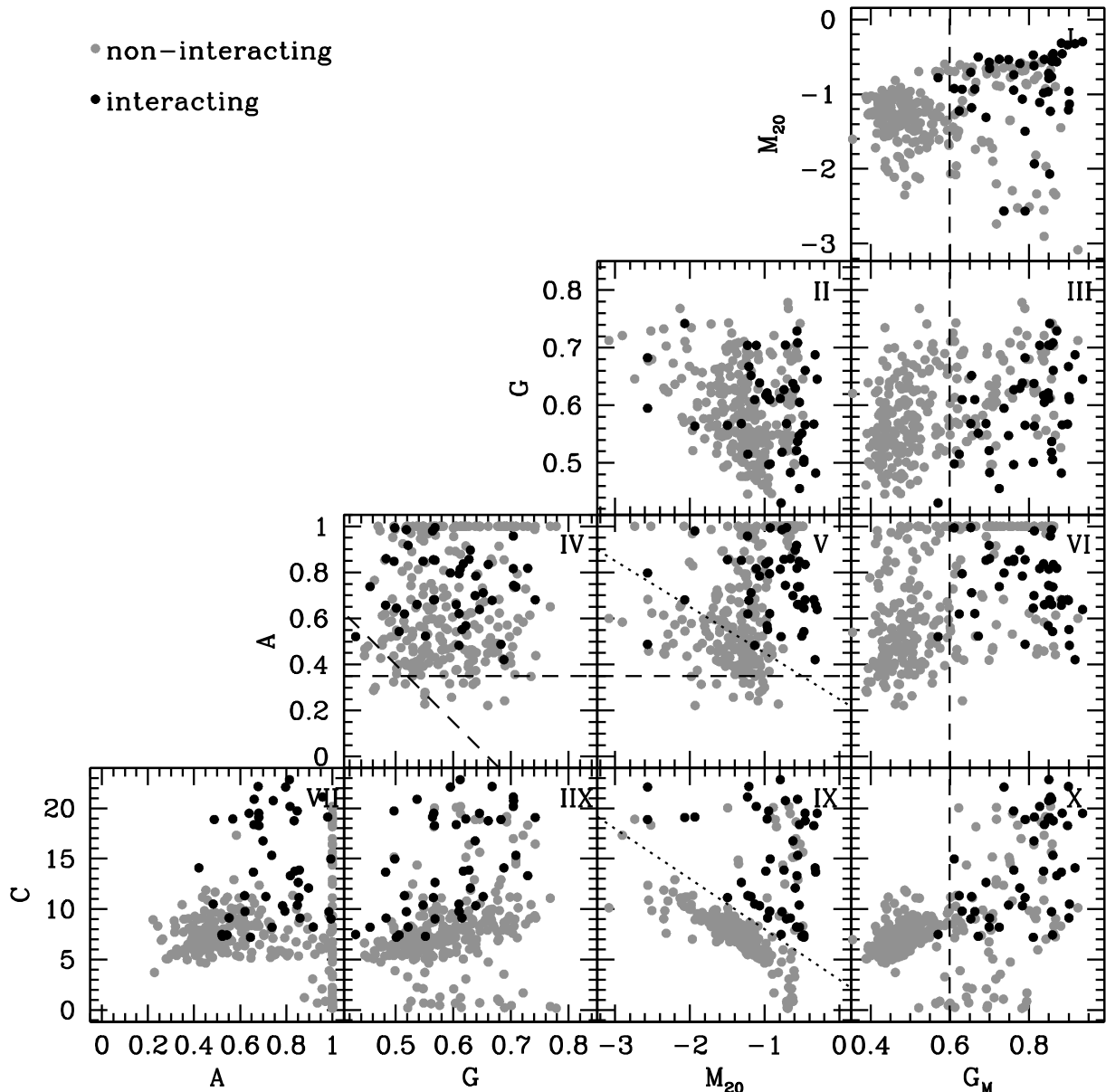
Figure 5. The distribution of morphological parameters, Concentration (C), Asymmetry (A), Gini (G) and the contribution to the second-order moment of the brightest 20 per cent of pixels (M_{20}), and the Gini coefficient of the second-order moment of the pixels (G_M). Merger selection criteria from the literature are marked with dashed lines in panel II (equation 8), panel IV (equations 7 and 9), and V and VI (equation 7). Our selection criteria from Holwerda et al. (2011c) are marked with dotted lines: the G_M criterion in panels I, III, VI and X (equation 10), the A–M_{20} criterion in panel V (equation 11) and the C–M_{20} criterion in panel IX (equation 12). Those objects selected by this last criterion (additionally requiring that Asymmetry is not extreme; $A \neq 1$) are marked in the plot for illustration. WHISP morphological values are given in Table A1 in the electronic version of the article.

variety of selection criteria (Table 3) and the merger rate from the Concentration–M_{20} criterion is $R_{\mathrm{mgr}}(\mathrm{morph}) = 6.8 \times 10^{-3}$ mergers Mpc^{-3} Gyr^{-1}.

Comparing the fraction found from galaxy pairs (7 per cent) with the number found from morphology (13 per cent), both seem to be in reasonable agreement, with the morphological selection on the high side. This is in line with the discrepancy found between pair selection and morphological selection as can be seen in Fig. 1. After factoring in the relative time-scales over which a merger is visible as a close pair (0.5 Gyr; Patton et al. 2000; Patton & Atfield 2008) or above the Concentration–M_{20} criterion (∼1 Gyr; Holwerda et al.

2011d), the volume merger rates agree very well: 7 and 6.8×10^{-3} mergers Gyr^{-1} Mpc^{-3} for paired and morphologically disturbed H I discs, respectively.

7 DISCUSSION

The WHISP sample represents only a very small volume of the Universe and the resulting merger fraction and rates are uncertain as a result of that. However, the consistency between our result and those from much larger samples such as the SDSS (e.g. Darg et al.

Table 3. Interaction fractions, merger visibility times and merger rates for the WHISP sample based on different morphological selection criteria.

Criterion	Mergers (No.)	f_{mrg} (per cent)	n_{mrg} (mergers Mpc^{-3})	T_{mrg} (Gyr)	R_{mgr} (mergers Gyr^{-1} Mpc^{-3})
pairs	15	7	0.0035	0.5	0.007
$A > 0.38$	221	65	0.032	1.85	0.017
$G > -0.115 \times M_{20} + 0.384$	178	53	0.026	0	...
$G > -0.4 \times A + 0.66$	235	69	0.034	0.15	0.23
$G_M > 0.6$	81	24	0.012	0.80	0.015
$A < -0.2 \times M_{20} + 0.25$	151	45	0.022	0.9	0.025
$C > -5 \times M_{20} + 3$	45	13	0.0066	0.97	0.0068

2010, see Fig. 1) is cause for optimism for the use of H I morphology as a tracer of the merger fraction and rate of galaxies.

Volume merger rates in the literature for the local Universe vary somewhat with sample and survey. Masjedi et al. (2006) find for luminous red galaxies in SDSS a volume merger rate of $R_{mgv} = 0.6 \times 10^4$ Gpc^{-3} Gyr$^{-1} = 1.7 \times 10^{-4} h^3$ Mpc^{-3} Gyr^{-1}. De Propris et al. (2007b) find for galaxies of all types in the Millennium Galaxy Catalogue (MGC) a volume merger rate of $R_{mgv} = 5.2 \pm 1.0 \times 10^{-4} h^3$ Mpc^{-3} Gyr^{-1}, and Patton & Atfield (2008) find a volume merger rate for all galaxy types based on SDSS and MGC of $R_{mgv} = 1.4 \pm 0.1 \times 10^{-4} h^3$ Mpc^{-3} Gyr^{-1} for *major* mergers. In contrast, we find a volume merger rate of R_{mgr}(morph) $= 2 \times 10^{-3}$ mergers h^3 Mpc^{-3} Gyr^{-1} ($h = 0.73$ or $H_0 = 73$ km s^{-1} Mpc^{-1}), an order of magnitude more than those above. Since our merger fractions are similar within a factor of 2 to those in the literature for the local Universe, the issue for the volume merger rate would have to be the inferred WHISP volume, the time-scale or a bias in the selection of galaxies.

The merger time-scale is unlikely to be the issue. The visibility time of the merger starts earlier in H I than in the stellar perspective but it is not substantially different from what other authors have found. Substituting any other visibility time-scale from the literature for morphological or pair selection would not reduce the merger rate (selection times are typically less than or equal to ~1 Gyr). We are more sensitive to minor mergers and the implied shorter visibility time-scales but this is unlikely to be an order of magnitude effect.

Alternatively, we may have to consider the possibility that the morphologically disturbed galaxies are not all gravitationally disturbed but may suffer from effects unique to the gas perspective,

for example ram-pressure stripping affecting the appearance of the H I disc. Compared to the observed fraction of mergers from other sources (e.g. Darg et al. 2010, for the SDSS), this is of the order of a factor of 2 discrepancy. The agreement between volume merger rates from WHISP from the pairs and morphology contradicts this, however.

The WHISP volume estimate is a likely source of the discrepancy as it is the most uncertain of our numbers. However, even with the naive, larger estimate of the WHISP volume (18×10^3 Mpc^3), this is only a factor of 3, not an order of magnitude.

The WHISP selection process favours late-type galaxies (Fig. 2) and local small irregular galaxies (to complement the spirals) and it was never intended as a volume-limited sample. Hence, an intentional or unintentional selection bias may well have been introduced. Mergers identifiable by their morphology are more likely to happen to the gas-rich late-types and the irregulars are confined to a local – smaller – volume, and many of them will be tidally affected. The H I perspective is likely to be more sensitive to unequal-mass mergers as these can be identified much more readily (the contrast in gas surface densities is not as great as it is in stellar surface brightness). Lotz et al. (2010b) point out how one expects a much higher merger fraction in lower-mass systems, and Patton & Atfield (2008) point out that a factor of 2 discrepancy can easily be expected if lower mass systems are included in even a pair statistical analysis. In addition, Lotz et al. (2010a) and Conselice (2009) identify that gas-rich mergers are the most easily identified by their morphology.

Therefore, we suspect our result points to a higher merger fraction and volume merger rate for spirals and irregulars in the local Universe, and less to a gross error in our WHISP volume, the merger
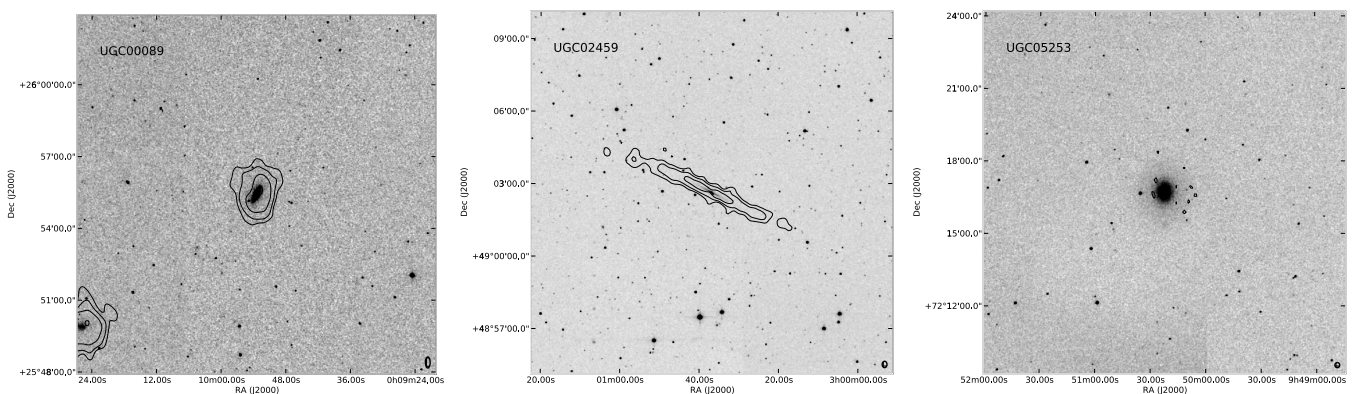
Figure 6. Three random examples of the galaxies selected by the Concentration–M_{20} criterion (equation 12). The grey-scale image is the 2MASS K-band image and the contours are WHISP column density contours at 2.5, 5, 10 and 20 $\times 10^{20}$ atoms arcsec^{-2}. The full set of galaxies selected by this criterion is shown in the Appendix (see Supporting Information).

fraction or the merger time-scale. If this is the case, merger fractions and rates for at least these types may not evolve with redshift as dramatically as previously thought. However, to confirm this, one would need a volume-limited large H I survey with sufficient resolution and sensitivity for both morphological selection and an accurate pair identification.

The H I perspective can be reliably used in the local Universe ($z \sim 0$), where a spatial resolution can be achieved in large, all-sky surveys [e.g. WALLABY on ASKAP (Koribalski et al., in preparation) and WNSHIS on WSRT (Józsa et al., in preparation)], but any morphological identification of interacting gas discs at higher redshift will have to wait for SKA. The resolution of the Pathfinder instruments (MeerKAT and ASKAP) may well be enough to identify close pairs in the proposed deep H I surveys [DINGO[3] on ASKAP (Meyer 2009; Meyer et al., in preparation) and LADUMA[4] with MeerKAT (Holwerda & Blyth 2010; Holwerda et al. 2011a, Holwerda et al., in preparation)].

8 CONCLUSIONS

In this paper, we explored the merger fraction and rate based on H I observations of the WHISP sample of galaxies. The sample is still small compared to other local references based on, for instance, the SDSS or the MGC (De Propris et al. 2005) but provides us with an indication of how well the H I surveys of the near future will perform in this respect. From the quantified morphologies of the WHISP column density maps, we conclude the following.

(1) The merger fraction in the WHISP sample is 7 per cent based on pairs, and 13 per cent based on disturbed morphology. These percentages are consistent if one takes into account how long a merger is visible as a close pair of galaxies and how long it is visible as a morphologically disturbed H I disc.

(2) Assuming the representative volume of the WHISP sample is 6835 Mpc^3, and a merger visibility time-scale of 1 Gyr, the merger rate for our selection criterion is $R_{mgr}(\text{morph}) = 6.8 \times 10^{-3}$ mergers Gyr^{-1} Mpc^{-3} in the local Universe, very close to the value of $R_{mgr}(\text{pairs}) = 7 \times 10^{-3}$ mergers Gyr^{-1} Mpc^{-3} for galaxy pairs in WHISP.

(3) While the WHISP merger fractions and especially rates mutually agree, the merger rates are much higher than those reported in the literature. Selection effects in the WHISP survey, preferring dwarf and irregulars, rather than a gross error in the WHISP volume, could well account for the difference as well as variation in the quality of the WHISP maps across the sample. Upcoming, volume-limited H I surveys should provide an accurate measurement of the local merger rate from both H I morphology and close pairs.

9 FUTURE WORK

The 21 cm window on the Universe is set to revolutionize our understanding of the merger rate of spiral and irregular galaxies as three independent measures of merging or gravitational interaction are available in the data: H I morphology, kinematic signatures in H I of interaction (e.g. lopsidedness of the profile, non-circular motions and an irregular velocity field) and the easy detection of physically close companions in the H I data cube.

Planned H I surveys with the SKA Pathfinder instruments include an all-sky survey (WALLABY with ASKAP and WNSHIS with WSRT/APERTIF), and a medium deep survey to $z \sim 0.4$ (DINGO) with ASKAP, and an extremely deep survey (LADUMA) with MeerKAT. Combined, these will revolutionize the volume probed with H I and help to shed light on the merger fraction using all three tracers: morphological, dynamic and pair identification in the local Universe surveys, and dynamical and close pair identification out to higher redshift.

REFERENCES

Arp H., 1973, ApJ, 185, 797
Bertin E., Arnouts S., 1996, A&AS, 117, 393
Booth R. S., de Blok W. J. G., Jonas J. L., Fanaroff B., 2009, preprint (arXiv:0910.2935)
Bridge C. R. et al., 2007, ApJ, 659, 931
Bridge C. R., Carlberg R. G., Sullivan M., 2010, ApJ, 709, 1067
Carilli C. L., Rawlings S., 2004, New Astron. Rev., 48, 979
Cassata P. et al., 2005, MNRAS, 357, 903
Chung A., van Gorkom J. H., Kenney J. D. P., Crowl H., Vollmer B., 2009, AJ, 138, 1741 (Erratum: 2010, AJ, 139, 2716)
Conselice C. J., 2003, ApJS, 147, 1
Conselice C. J., 2009, MNRAS, 399, L16
Conselice C. J., Bershady M. A., Dickinson M., Papovich C., 2003, AJ, 126, 1183
Conselice C. J., Blackburne J. A., Papovich C., 2005, ApJ, 620, 564
Conselice C. J., Bundy K., U V., Eisenhardt P., Lotz J., Newman J., 2008, MNRAS, 383, 1366
Conselice C. J., Yang C., Bluck A. F. L., 2009, MNRAS, 361
Cotton W. D., Condon J. J., Arbizzani E., 1999, ApJS, 125, 409
Cox T. J., Dutta S. N., Di Matteo T., Hernquist L., Hopkins P. F., Robertson B., Springel V., 2006a, ApJ, 650, 791
Cox T. J., Jonsson P., Primack J. R., Somerville R. S., 2006b, MNRAS, 373, 1013
Darg D. W. et al., 2010, MNRAS, 401, 1043
de Blok W. J. G., Jonas J., Fanaroff B., Holwerda B. W., Bouchard A., Blyth S., van der Heyden K., Pirzkal N., 2009, in Serra P., Heald G., eds, Panoramic Radio Astronomy: Wide field 1–2 GHz Research on Galaxy Evolution. SISSA, http://pos.sissa.it
De Propris R., Liske J., Driver S. P., Allen P. D., Cross N. J. G., 2005, AJ, 130, 1516
De Propris R., Conselice C. J., Liske J., Driver S. P., Patton D. R., Graham A. W., Allen P. D., 2007a, ApJ, 666, 212
De Propris R., Conselice C. J., Liske J., Driver S. P., Patton D. R., Graham A. W., Allen P. D., 2007b, ApJ, 666, 212
de Ravel L. et al., 2009, A&A, 498, 379
Genel S., Genzel R., Bouché N., Naab T., Sternberg A., 2009, ApJ, 701, 2002
Hibbard J. E., van Gorkom J. H., Rupen M. P., Schiminovich D., 2001, in Hibbard J. E., Rupen M., van Gorkom J. H., eds, ASP Conf. Ser. Vol. 240, Gas and Galaxy Evolution. Astron. Soc. Pac., San Francisco, p. 657
Holwerda B. W., 2005, preprint (astro-ph/0512139)

---

[3] Deep Investigations of Neutral Gas in Origins.
[4] Looking At the Distant Universe with the MeerKAT Array.

Holwerda B., Blyth S., 2010, in Heald G., ed., ISKAF2010 Science Meeting. SISSA, http://pos.sissa.it

Holwerda B. W., de Blok W. J. G., Bouchard A., Blyth S., van der Heyden K., Pirzkal N., 2009, in Serra P., Heald G., eds, Panoramic Radio Astronomy: Wide field 1–2 GHz Research on Galaxy Evolution. SISSA, http://pos.sissa.it

Holwerda B. W., Blyth S., Baker A. J., MeerKAT Deep HI Survey Team, 2011a, BAAS, 43, 433.17 [American Astronomical Society Meeting Abstracts 217]

Holwerda B. W., Pirzkal N., de Blok W. J. G., Bouchard A., Blyth S.-L., van der Heyden K. J., Elson E. C., 2011b, MNRAS, in press (doi:10.1111/j.1365-2966.2011.18938.x)

Holwerda B. W., Pirzkal N., de Blok W. J. G., Bouchard A., Blyth S.-L., van der Heyden K. J., Elson E. C., 2011c, MNRAS, in press (doi:10.1111/j.1365-2966.2011.17683.x)

Holwerda B. W., Pirzkal N., Cox T. J., de Blok W. J. G., Weniger J., Bouchard A., Blyth S.-L., van der Heyden K. J., 2011d, MNRAS, in press (doi:10.1111/j.1365-2966.2011.18940.x)

Holwerda B. W., Pirzkal N., de Blok W. J. G., van Driel W., 2011e, MNRAS, in press (doi:10.1111/j.1365-2966.2011.18662.x)

Hopkins P. F. et al., 2010, ApJ, 724, 915

Jogee S. et al., 2009, ApJ, 697, 1971

Johnston S., 2007, in Beswick R., ed., From Planets to Dark Energy: the Modern Radio Universe. SISSA, http://pos.sissa.it, p. 6

Johnston S. et al., 2007, Publ. Astron. Soc. Australia, 24, 174

Johnston S. et al., 2008, Exp. Astron., 22, 151

Johnston S., Feain I. J., Gupta N., 2009, in Saikia D. J., Green D. A., Gupta Y., Venturi T., eds, ASP Conf. Ser. Vol. 407, The Low-Frequency Radio Universe. Astron. Soc. Pac., San Francisco, p. 446

Jonas J., 2007, in Beswick R., ed., From Planets to Dark Energy: the Modern Radio Universe. SISSA, http://pos.sissa.it, p. 7

Kartaltepe J. S. et al., 2007, ApJS, 172, 320

Kleinmann S. G. et al., 1994, Exp. Astron., 3, 65

Le Fèvre O. et al., 2000, MNRAS, 311, 565

Lin L. et al., 2004, ApJ, 617, L9

Lin L. et al., 2008, ApJ, 681, 232

Lintott C. J. et al., 2008, MNRAS, 389, 1179

Lotz J. M., Primack J., Madau P., 2004, AJ, 128, 163

Lotz J. M. et al., 2008, ApJ, 672, 177

Lotz J. M., Jonsson P., Cox T. J., Primack J. R., 2010a, MNRAS, 404, 590

Lotz J. M., Jonsson P., Cox T. J., Primack J. R., 2010b, MNRAS, 404, 575

Masjedi M. et al., 2006, ApJ, 644, 54

Meyer M., 2009, in Serra P., Heald G., eds, Panoramic Radio Astronomy: Wide field 1–2 GHz Research on Galaxy Evolution. SISSA, http://pos.sissa.it

Napier P. J., 2006, in Backer D. C., Moran J. M., Turner J. L., eds, ASP Conf. Ser. Vol. 356, Revealing the Molecular Universe: One Antenna is Never Enough, Astron. Soc. Pac., San Francisco, p. 65

Nilson P., 1973, Uppsala General Catalogue of Galaxies. Acta Universitatis Upsaliensis. Nova Acta Regiae Societatis Scientiarum Upsaliensis – Uppsala Astronomiska Observatoriums Annaler

Noordermeer E., 2006, PhD thesis, AA, Groningen: Rijksuniversiteit

Noordermeer E., van der Hulst J. M., Sancisi R., Swaters R. A., van Albada T. S., 2005a, A&A, 442, 137

Noordermeer E., van der Hulst J. M., Sancisi R., Swaters R. A., van Albada T. S., 2005b, A&A, 442, 137

Oosterloo T., Verheijen M., van Cappellen W., Bakker L., Heald G., Ivashina M., 2009, preprint (arXiv e-prints)

Patton D. R., Atfield J. E., 2008, ApJ, 685, 235

Patton D. R., Pritchet C. J., Yee H. K. C., Ellingson E., Carlberg R. G., 1997, ApJ, 475, 29

Patton D. R., Carlberg R. G., Marzke R. O., Pritchet C. J., da Costa L. N., Pellegrini P. S., 2000, ApJ, 536, 153

Patton D. R. et al., 2002, ApJ, 565, 208

Paturel G., Petit C., Prugniel P., Theureau G., Rousseau J., Brouty M., Dubois P., Cambrésy L., 2003a, A&A, 412, 45

Paturel G., Petit C., Prugniel P., Theureau G., Rousseau J., Brouty M., Dubois P., Cambrésy L., 2003b, A&A, 412, 45

Robaina A. R. et al., 2009, ApJ, 704, 324

Scarlata C. et al., 2007, ApJS, 172, 406

Springob C. M., Haynes M. P., Giovanelli R., Kent B. R., 2005, ApJS, 160, 149

Swaters R. A., Balcells M., 2002, A&A, 390, 863

Swaters R. A., van Albada T. S., van der Hulst J. M., Sancisi R., 2002a, A&A, 390, 829

Swaters R. A., van Albada T. S., van der Hulst J. M., Sancisi R., 2002b, A&A, 390, 829

van der Hulst J. M., 2002, in Taylor A. R., Landecker T. L., Willis A. G., eds, ASP Conf. Ser. Vol. 276, Seeing Through the Dust: The Detection of HI and the Exploration of the ISM in Galaxies. Astron. Soc. Pac., San Francisco, p. 84

van der Hulst J. M., van Albada T. S., Sancisi R., 2001, in Hibbard J. E., Rupen M., van Gorkom J. H., eds, ASP Conf. Ser. Vol. 240, Gas and Galaxy Evolution. Astron. Soc. Pac., San Francisco, p. 451

Verheijen M. A. W., Oosterloo T. A., van Cappellen W. A., Bakker L., Ivashina M. V., van der Hulst J. M., 2008, in Minchin R., Momjian E., eds, AIP Conf. Ser. Vol. 1035, The Evolution of Galaxies Through the Neutral Hydrogen Window. Am. Inst. Phys., New York, p. 265

Vorontsov-Velyaminov B. A., Noskova R. I., Arkhipova V. P., 2001, Astron. Astrophys. Trans., 20, 717

Zwaan M. A., 2000, PhD thesis, Groningen: Rijksuniversiteit

Zwaan M. A., Briggs F. H., Sprayberry D., Sorar E., 1997, ApJ, 490, 173

SUPPORTING INFORMATION

Additional Supporting Information may be found in the online version of this article:

Table A1. Morphological parameters for the complete WHISP sample.

Figure A1. Galaxies selected as mergers by the Concentration–M_{20} selection criterion.

Please note: Wiley-Blackwell are not responsible for the content or functionality of any supporting materials supplied by the authors. Any queries (other than missing material) should be directed to the corresponding author for the article.

This paper has been typeset from a TEX/LATEX file prepared by the author.